

Salicylic Acid and Analogs: Diamagnetic Chemical Exchange Saturation Transfer (diaCEST) Magnetic Resonance Imaging (MRI) Contrast Agents with Highly Shifted Exchangeable Protons

Xing Yang^{1#}, Xiaolei Song^{1,2#}, Yuguo Li^{1,2}, Guanshu Liu^{1,2}, Sangeeta Ray¹, Martin G. Pomper^{1*},
Michael T. McMahon^{1,2*}

¹Russell H. Morgan Department of Radiology The Johns Hopkins University School of Medicine, Baltimore, Maryland, USA.

²F.M. Kirby Research Center for Functional Brain Imaging, Kennedy Krieger Institute, Baltimore, Maryland, USA.

SUPPORTING INFORMATION

1.	GENERAL	S1
2.	¹H-NMR SPECTRUM OF SALICYLIC ACID IN WATER	S2
3.	Z-SPECTRA OF SALICYLIC ACID AT DIFFERENT PH AND CONCENTRATION	S3
4.	PROTON EXCHANGE RATE OF SALICYLIC ACID AT DIFFERENT PH	S4
5.	Z-SPECTRA OF SALICYLIC ACID ANALOGUES	S6
6.	IN VIVO DATA	S8
7	REFERENCE	S12

1. GENERAL

Phantom Preparation: All compounds were purchased from Sigma Aldrich (St. Louis, MO). Samples were dissolved in 0.01M phosphate-buffered saline (PBS) at the desired concentrations, and titrated using high concentration HCl/NaOH to the desired pH. The solutions were placed into 1 mm glass capillaries and assembled in a holder for CEST MR imaging. The samples were kept in 37°C during imaging. Phantom CEST experiments were taken on a Bruker 11.7 Tesla vertical MR scanner, using a 20 mm birdcage transmit/receive coil. CEST images were acquired using a RARE (RARE = 8) sequence with CW saturation pulse length of 3 seconds and saturation field strength (ω_1) from 1.2 μ T to 14.4 μ T. The CEST Z-spectra were acquired by incrementing saturation frequency every 0.3 ppm from -15 to 15 ppm for phantoms; TR = 6 s, effective TE = 17 ms, matrix size = 64x48 and slice thickness of 1.2 mm.

Animal Imaging: BALB/c mice weighing 20–25 g (Charles River Laboratories, Wilmington, MA) were maintained under specific pathogen free conditions in the animal facility of Johns Hopkins University. For MRI, mice were anesthetized by using 0.5–2% isoflurane and placed in a 23 mm transmit/receive mouse coil. Breath rate was monitored throughout in vivo MRI experiments using a respiratory probe. A 60 μ L volume of a 0.25 M salicylic acid solution in PBS (pH 7) was slowly injected *via* a catheter into the tail vein. In vivo images were acquired on a Bruker Biospec 11.7 T horizontal MR scanner, with one axial slice (1.5 mm thick) crossing both renal centre chosen for CEST screening. CEST images were acquired both pre- and post-injection. Image parameters were similar to those for the phantom except for TR/TE = 5s/15 ms, with optimized $\omega_1 = 7.2 \mu$ T.

2. ¹H-NMR SPECTRUM OF SALICYLIC ACID IN WATER

Salicylic acid (**1**) was dissolved in 0.01 M PBS with 10% deuterium oxide at the concentration of 25 mM and titrated with HCl/NaOH to pH 7.0. The ¹H-NMR was acquired on a 500M Bruker NMR spectrometer at room temperature. The spectra and proton assignment are shown in Figure S1. The C2-OH exchangeable proton was clearly observed at chemical shift 14 ppm from TMS.

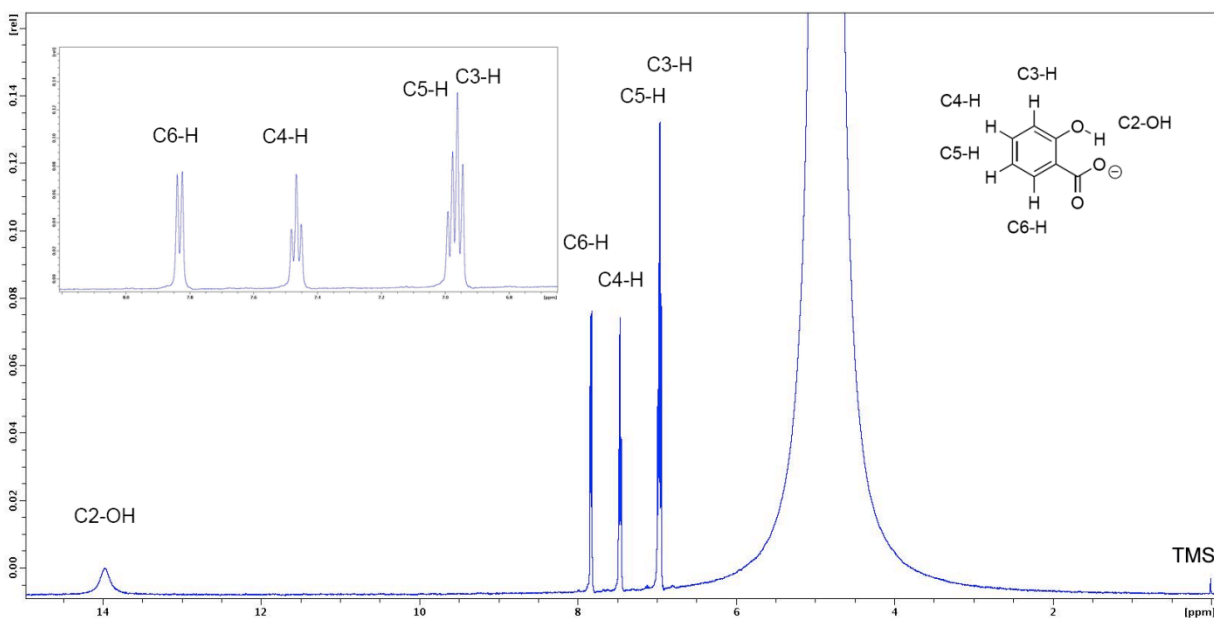


Figure S1. ¹H-NMR of salicylic acid (**1**) in water.

3. Z-SPECTRA OF SALICYLIC ACID AT DIFFERENT pH AND CONCENTRATION

A) The effect of pH on the contrast of salicylic acid (**1**) was tested at a concentration of 25 mM, $\omega_1 = 7.2 \mu\text{T}$. The Z-spectra and MTR_{asym} of pH 5.8, 6.5, 6.8, 7.2, 7.6, 8.1, 11.7 were collected and shown in Figure S2. Maximal contrast was observed between pH 6.5 and 7.0.

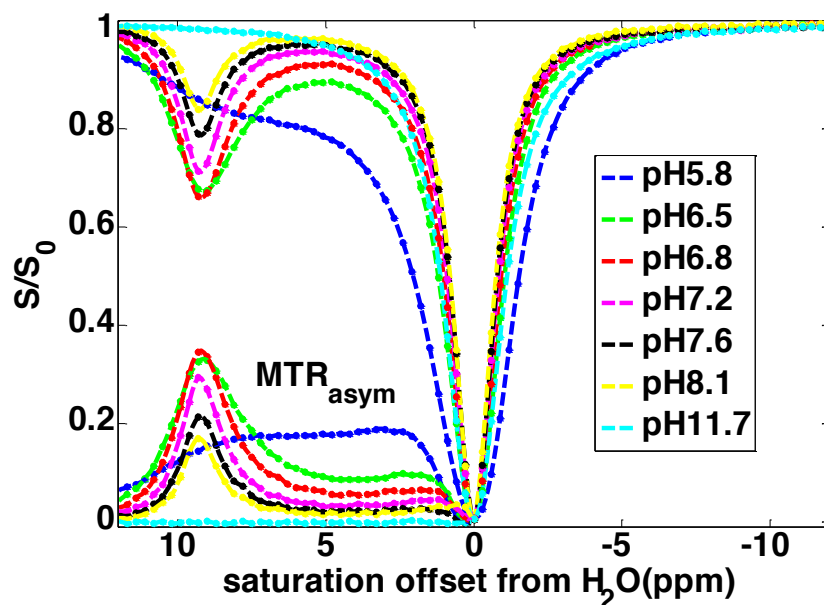


Figure S2. pH effect on the contrast of salicylic acid (**1**)

B) The concentration dependence of the contrast of salicylic acid (**1**) at pH 7.3-7.4 was measured at a saturation field strength (ω_1) = 7.2 μT . The Z-spectra and MTR_{asym} spectra at concentrations 1.5 mM, 3.1 mM, 6.3 mM, 12.5 mM, 25.0 mM and 50.0 mM were collected and are shown below. 4% contrast was obtained at 1.50 mM.

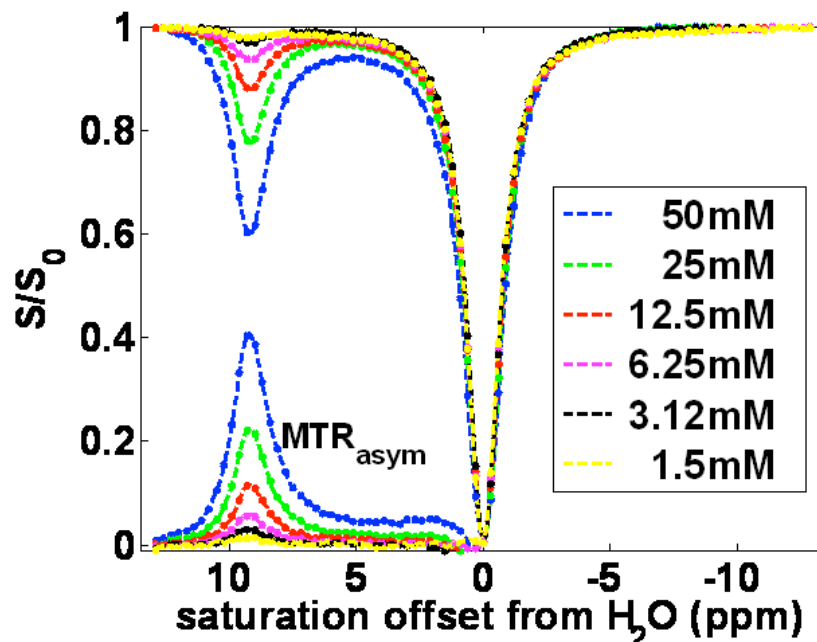


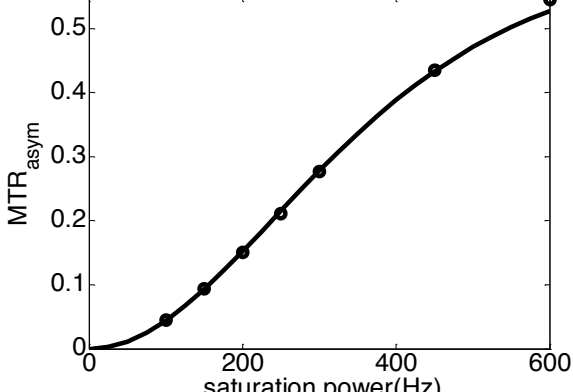
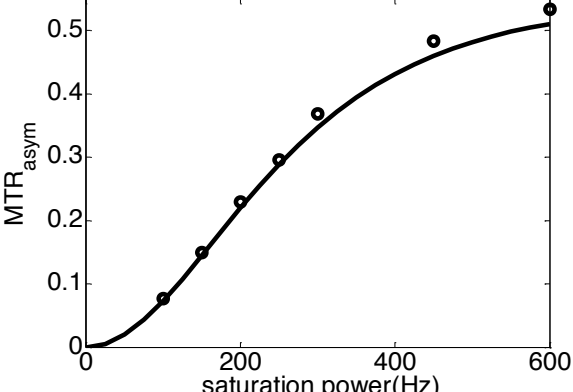
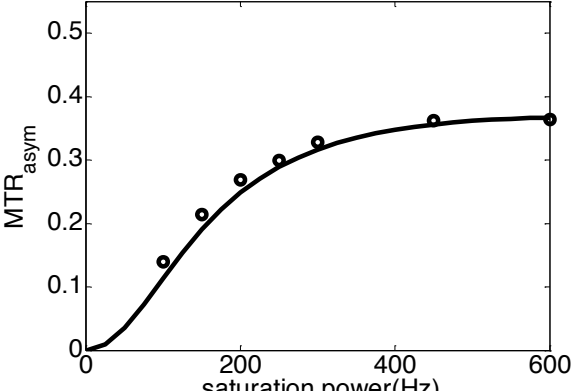
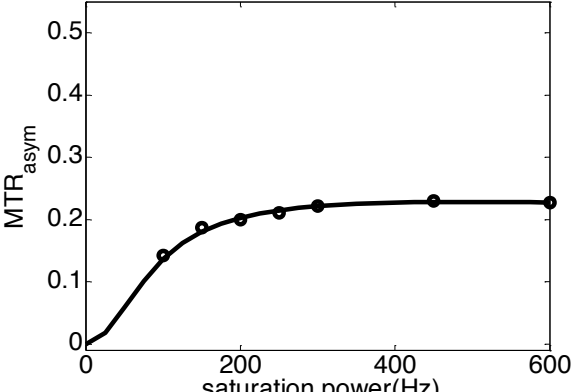
Figure S2. Concentration effect on the contrast of salicylic acid (**1**)

4. PROTON EXCHANGE OF SALICYLIC ACID AT DIFFERENT pH

QUESP datasets for salicylic acid (**1**) at 9.3 ppm were collected as a function of pH using $\omega_1 = 1.2 \mu\text{T}$, $2.4 \mu\text{T}$, $3.6 \mu\text{T}$, $5.4 \mu\text{T}$, $7.2 \mu\text{T}$, $10.8 \mu\text{T}$ and $11.4 \mu\text{T}$. The solvent to water exchange rate (k_{sw}) was calculated according to fitting to a 2-pool Bloch equation model.^[1] The parameters for all fitting were: $R_{1w} = 0.3$, $R_{2w} = 0.6$, $R_{1s} = 0.71$, $R_{2s} = 39$, $T_{\text{sat}} = 3\text{s}$. The results at pH 5.8, 6.2, 6.5, 7.0, 7.4 and 7.8 were summarized in Table S1.

Table S1. The calculated proton exchange rate of salicylic acid (**1**) at different pH.

entry	pH	QUESP fitting ^[1]	Exchange rate (k/sec.)
1	5.8		9.7

2	6.2	 <p>A line graph showing the relationship between saturation power (Hz) on the x-axis and MTR_{asym} on the y-axis. The x-axis ranges from 0 to 600 Hz with major ticks at 0, 200, 400, and 600. The y-axis ranges from 0 to 0.5 with major ticks at 0, 0.1, 0.2, 0.3, 0.4, and 0.5. The data points are connected by a smooth curve that starts at (0,0) and increases monotonically, reaching approximately 0.52 at 600 Hz.</p>	4.2
3	6.5	 <p>A line graph showing the relationship between saturation power (Hz) on the x-axis and MTR_{asym} on the y-axis. The x-axis ranges from 0 to 600 Hz with major ticks at 0, 200, 400, and 600. The y-axis ranges from 0 to 0.5 with major ticks at 0, 0.1, 0.2, 0.3, 0.4, and 0.5. The data points are connected by a smooth curve that starts at (0,0) and increases monotonically, reaching approximately 0.52 at 600 Hz.</p>	2.4
4	7.0	 <p>A line graph showing the relationship between saturation power (Hz) on the x-axis and MTR_{asym} on the y-axis. The x-axis ranges from 0 to 600 Hz with major ticks at 0, 200, 400, and 600. The y-axis ranges from 0 to 0.5 with major ticks at 0, 0.1, 0.2, 0.3, 0.4, and 0.5. The data points are connected by a smooth curve that starts at (0,0) and increases monotonically, reaching approximately 0.36 at 600 Hz.</p>	1.2
5	7.4	 <p>A line graph showing the relationship between saturation power (Hz) on the x-axis and MTR_{asym} on the y-axis. The x-axis ranges from 0 to 600 Hz with major ticks at 0, 200, 400, and 600. The y-axis ranges from 0 to 0.5 with major ticks at 0, 0.1, 0.2, 0.3, 0.4, and 0.5. The data points are connected by a smooth curve that starts at (0,0) and increases monotonically, reaching approximately 0.22 at 600 Hz.</p>	0.6

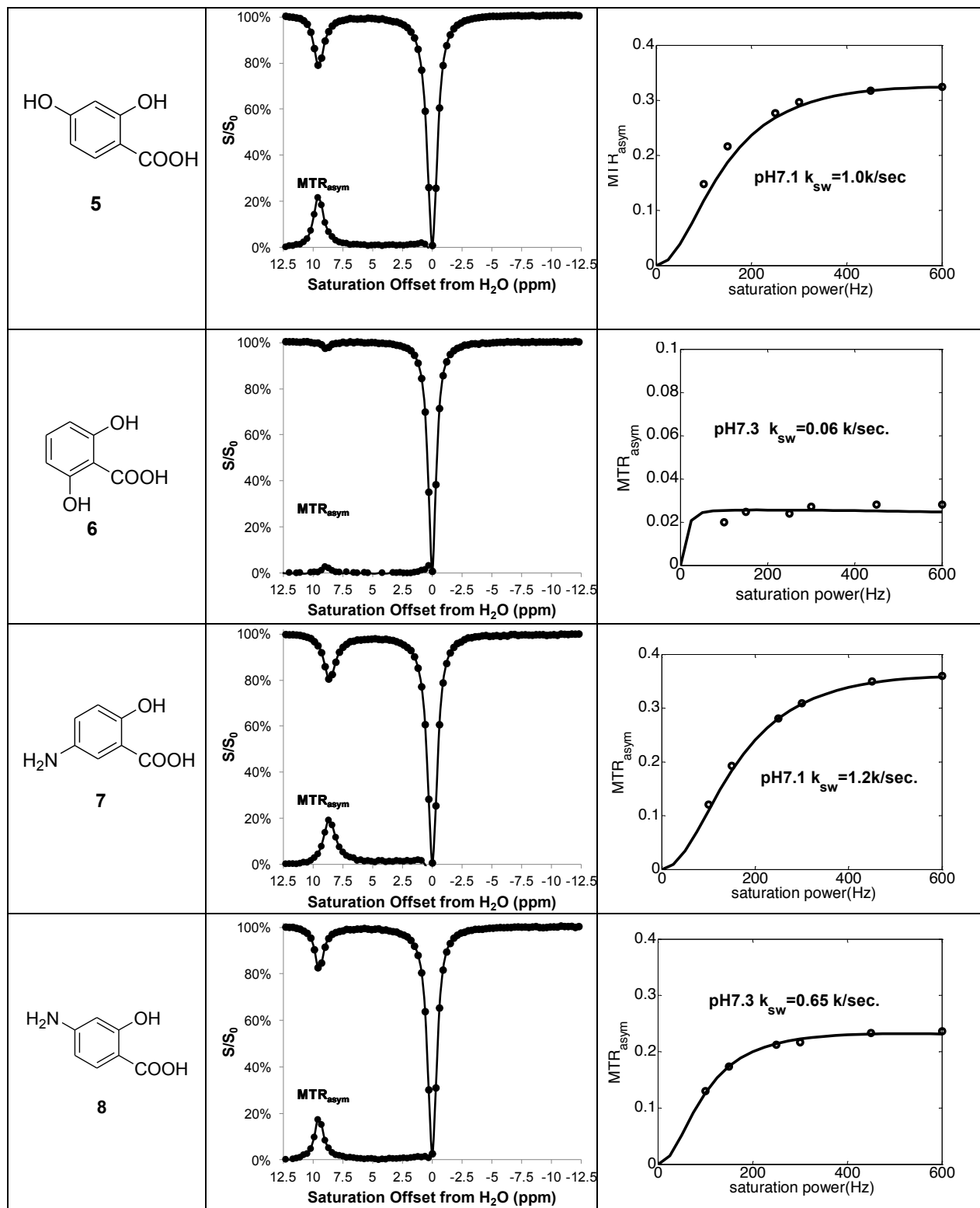
6	7.8		0.4
---	-----	--	-----

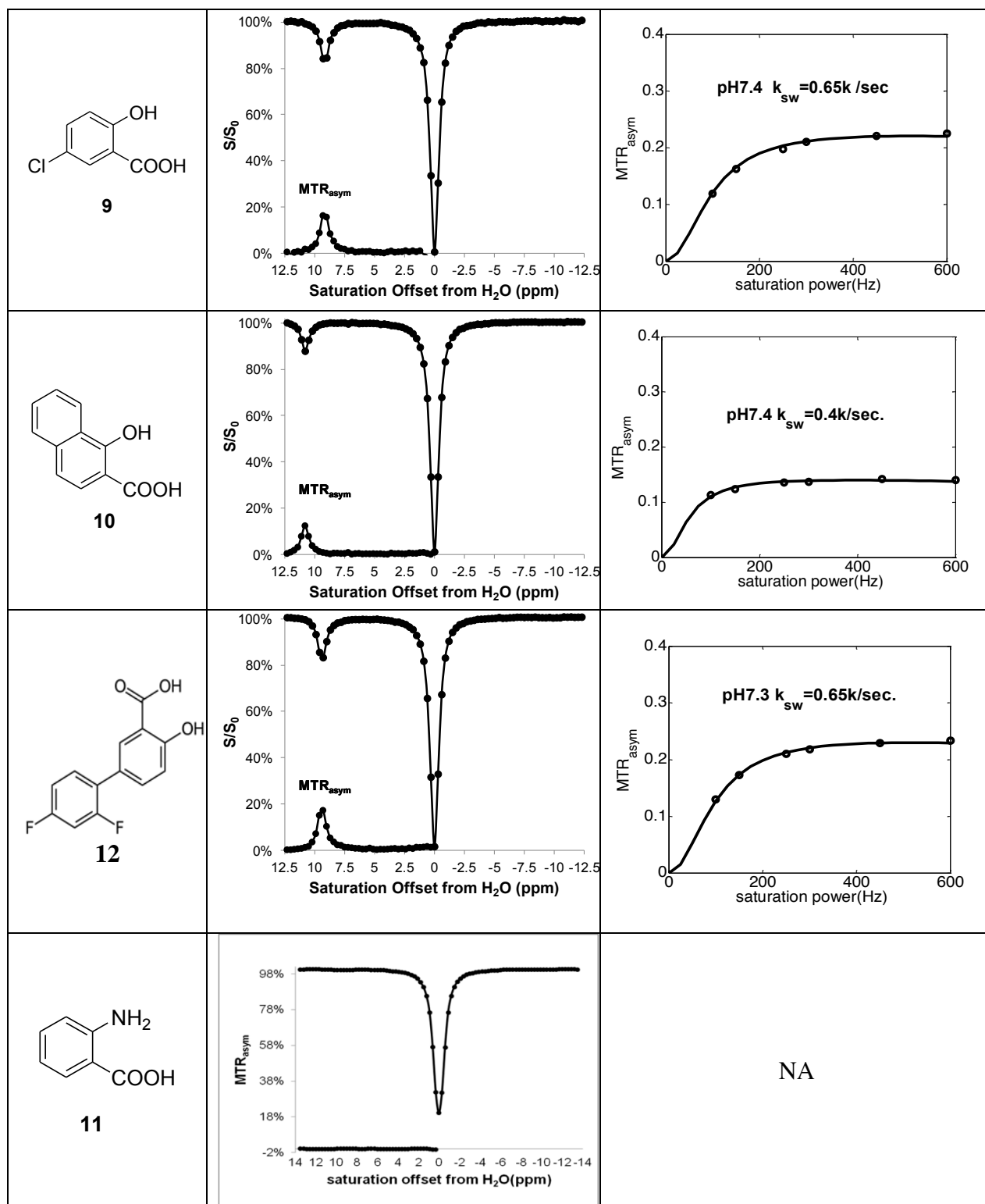
5. Z-SPECTRA OF SALICYLIC ACID ANALOGUES

25 mM salicylic acid analogs (**4** – **11**) were made at pH 7.1-7.4 and tested with the phantom condition as mentioned in general section. The Z-spectra were obtained by using $T_{\text{sat}} = 3$ sec, $\omega_1 = 3.6$ μT at 37 °C. The Z-spectra, MTR_{asym} and QUESP curve are listed in the Table S2.

Table S2. The Z-spectra and MTR_{asym} of salicylic acid analogs

Compound	Z-spectra and MTR_{asym}	Exchange rate fitting
 4		





6. IN VIVO DATA

A) *In vivo* data collection scheme 1

For the initial test, we started with an injection of 100 μl of 250 mM compound **1** solution into the mouse tail vein (i.v.), and acquired CEST images using a saturation field strength of 5.9 μT . A Z-spectrum was acquired before injection. For the dynamic CEST contrast measurements, we used a 6-offset scheme (± 9.6 ppm, ± 9.3 ppm, ± 9.0 ppm, 5 min temporal resolution) after i.v. injection to ensure robustness to B_0 inhomogeneity and high contrast-noise-ratio. The CEST contrast map was calculated with averaging over the 3 offsets (9.6 ppm, 9.3 ppm and 9.0 ppm). The kidney reached maximum CEST contrast at around 5 min, and then the contrast started decaying at 10 min. The Z-spectra are plotted in Figure S3, and the pre- and post- injection maps are shown in Table S3.

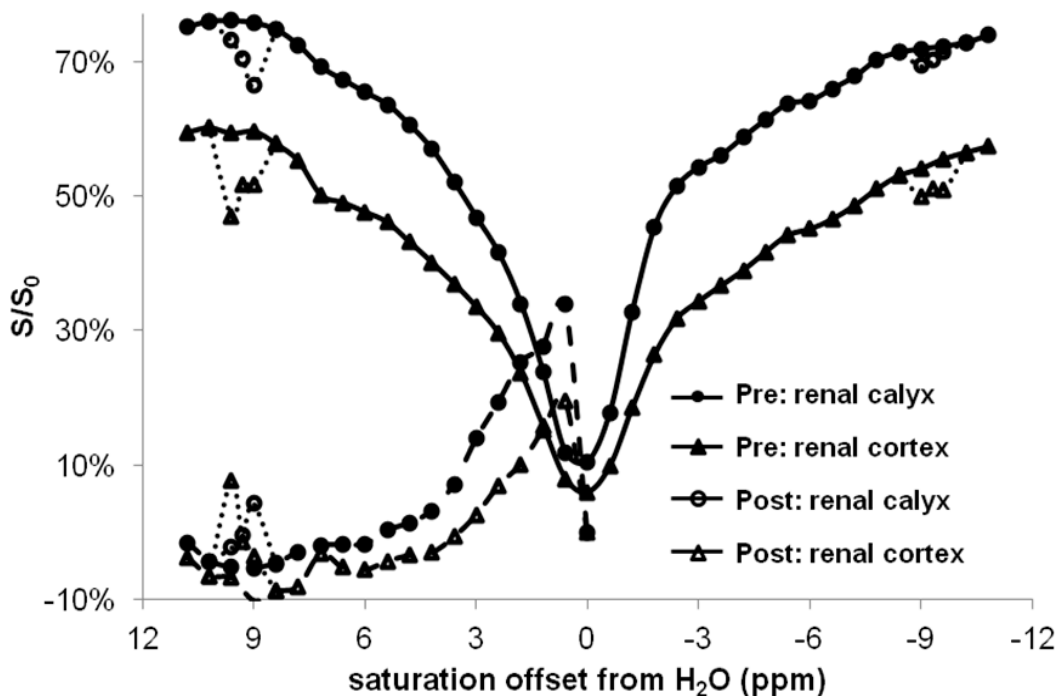
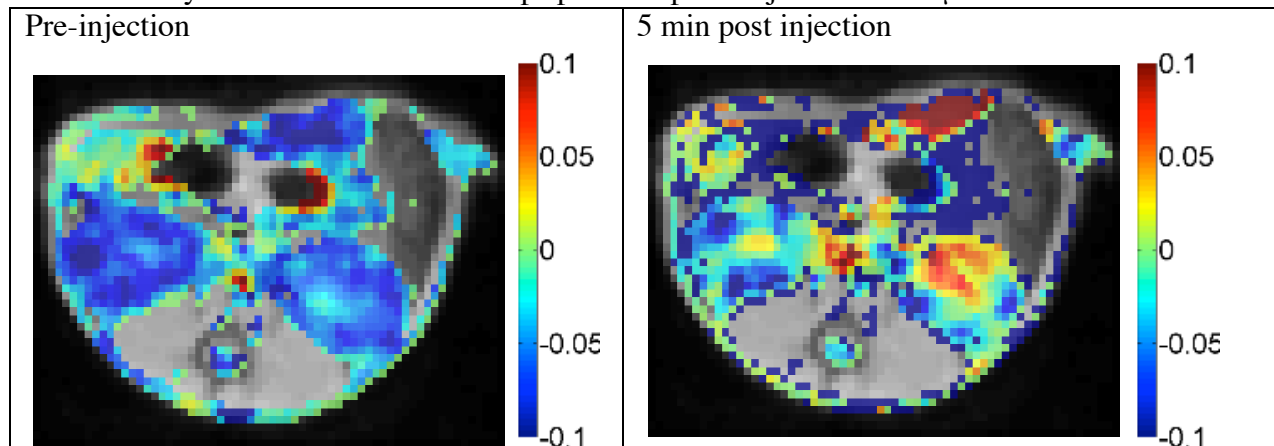
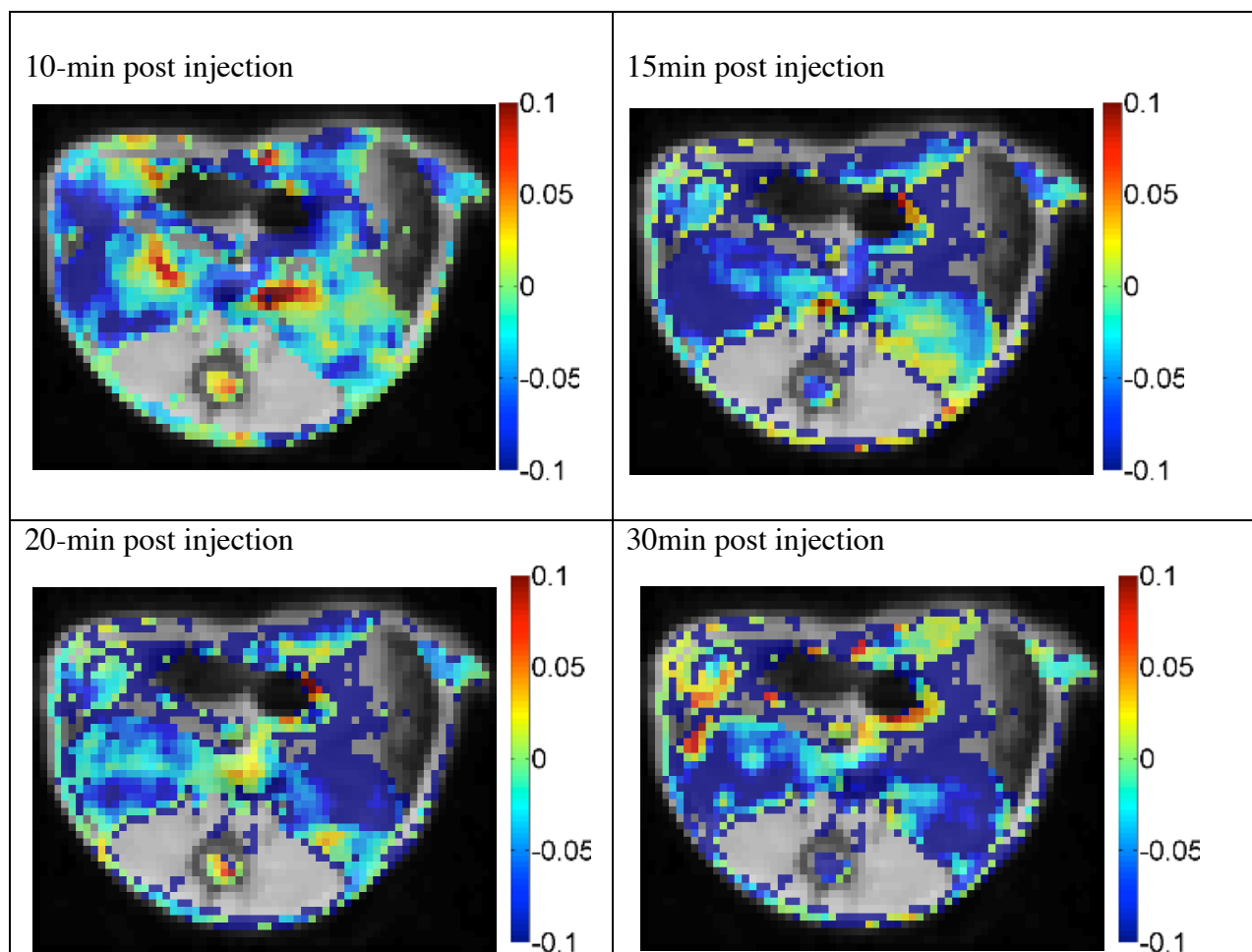


Figure S3. *In vivo* Z-spectra and MTR_{asym} spectra for renal calyx and cortex, acquired both pre-injection and at 5 min post-injection.

Table S3. Dynamic CEST contrast maps pre- and post- injection at 5.9 μT .

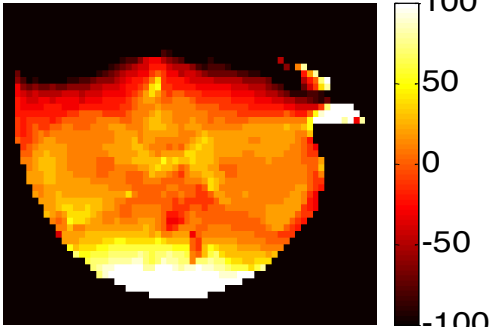
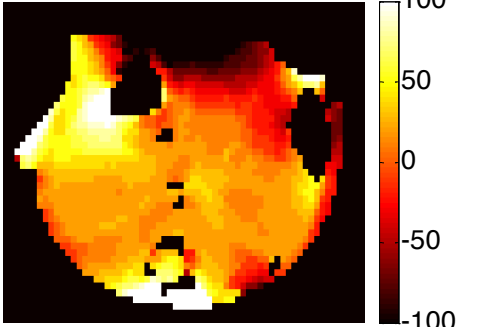
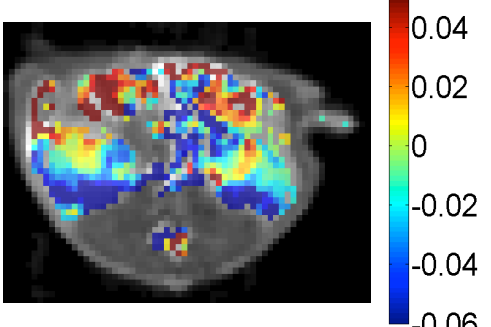
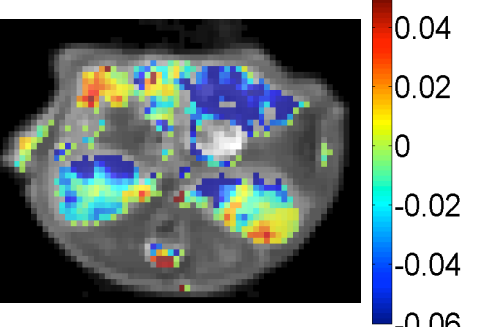
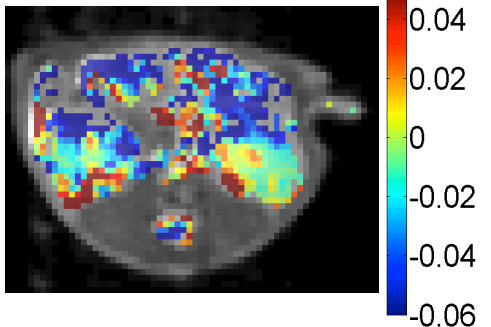
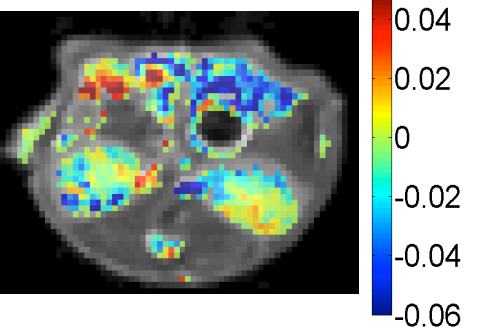
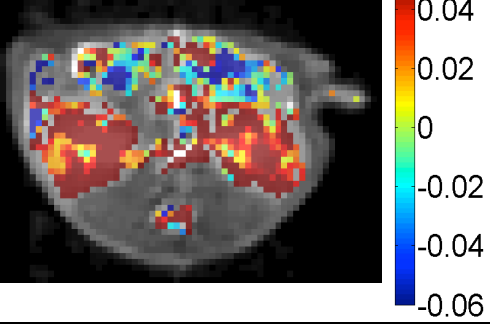
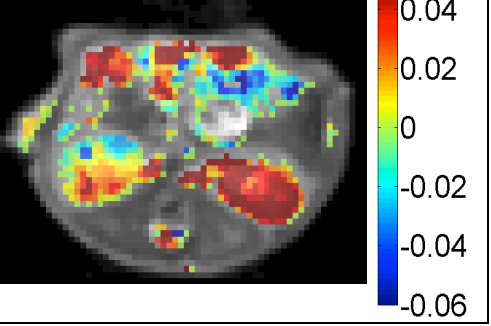


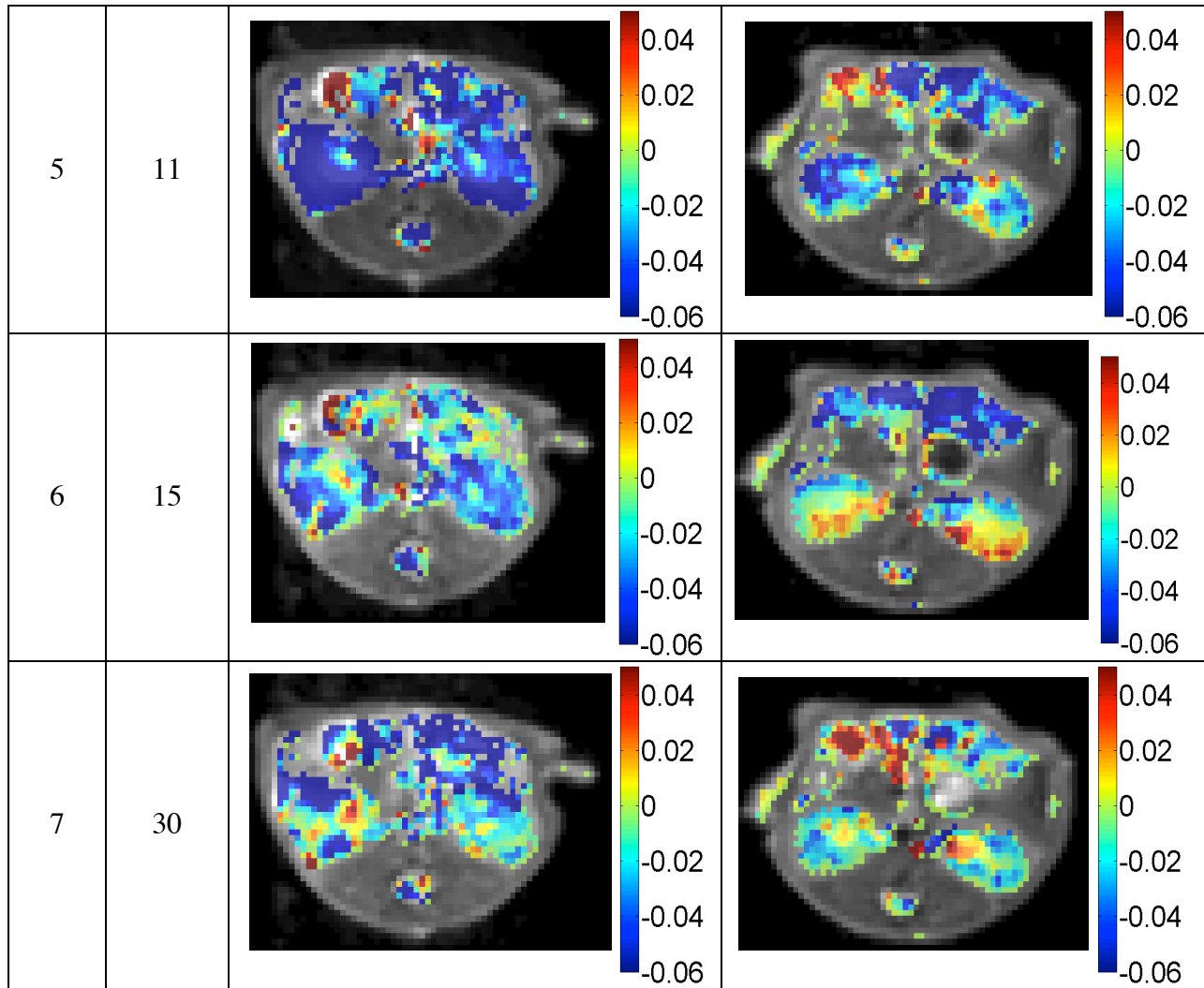


B) Scheme 2: Improved CEST imaging of kinetics:

According to the initial results in Figure S3 and Table S3, we modified the *in vivo* data collection scheme, in order to improve the kinetic data for compound **1** in the kidney. In addition, we further reduce the dose of agent to 60 μl of 250 mM solution. Instead of time consuming 5.9 μT 6-offset, we used 7.2 μT 2 offset at 9.3 ppm and -9.3 ppm for the dynamic CEST image acquisition. For the image post-processing, the CEST contrast maps at 9.3 ppm was smoothed by adding a 2x2 medium filter and overlapped to the saturation weighted image at -9.3 ppm. Images at every two adjacent time points were also averaged to increase the contrast-noise-ratio, with a temporal resolution of 3 min. For 2 mice, the dynamic contrast maps are shown in Table S4.

Table S4. The dynamic contrast maps for two mice

Entry	Time (min)	Mouse 1 (0309M2)	Mouse 2 (0311M3)
1	B0 Map		
2	0 Pre-inject		
3	3		
4	7		



7. REFERENCES

- [1] M. T. McMahon, A. A. Gilad, J. Zhou, P. Z. Sun, J. W. M. Bulte, P. C. M. van Zijl, *Magn. Reson. Med.* **2006**, *55*, 836-847
- [2] D. L. Longo, W. Dastru, G. Digilio, J. Keupp, S. Langereis, S. Lanzardo, S. Prestigio, O. Steinbach, E. Terreno, F. Uggeri, S. Aime, *Magn. Reson. Med.* **2011**, *65*, 202-211.;